Residual astigmatism prediction in cataract surgery: improvement strategies

Catarina Isabel Praefke Aires Coutinho
catarina.coutinho@tecnico.ulisboa.pt

Instituto Superior Técnico, Lisboa, Portugal

December 2021

Abstract

Cataract surgery is currently one of the most common interventions to restore visual acuity, where the associated astigmatism can be corrected by toric intraocular lens (IOL) implantation. Improving refractive outcomes by accurate and precise IOL power calculations is crucial to achieve optimal post-operative results matching the patients' expectations. For the minimization of residual astigmatism, linear regression-based nomograms between the Lenstar® keratometric astigmatism and the Cassini® total corneal astigmatism were developed, considering the posterior corneal effect and reducing the prediction error. Also, astigmatism variations were observed between center and peripheric zones, with a decrease of the toric IOL power determined to be implanted towards the periphery. Distinct numbers of measurements at different surgery-related stages for diverse measurement modalities evidenced no differences regarding the error in refractive astigmatism. Keratometric and total corneal astigmatism optimization was evaluated for linear and non-linear machine learning estimators in a three-step exploratory analysis, encountering several biometric parameters. Linear and tree-based models showed promising results for the reduction of the error in refractive astigmatism, requiring more testing data. Tailored IOL power calculations via ray-tracing, in diverse scenarios, were enabled by the implementation of an astigmatic pseudophakic eye model with a created generic simulated toric IOL, suitable for patient-specific data incorporation, highlighting the spherical power tenderness to the IOL position estimations and the cylindrical power relation with the posterior cornea.
Keywords: Cataract Surgery, Toric Intraocular Lens, Keratometric Astigmatism, Total Corneal Astigmatism, Residual Astigmatism, Prediction Error

1. Introduction

Vision, one of the human five senses, is of upmost importance for the perception of the surrounding environment, through complex and not yet fully understood mechanisms carried out by the articulation of eye and brain. As any other organ, the eye is subjected to defects, as cataracts, the opacification of the natural lens, considered the leading cause of blindness. Currently, with the increase of life expectancy, along with the continuous improvement of surgical techniques, cataract surgery is a common procedure in developed countries and regarded as one of the most effective and successful interventions to restore visual quality [1]. A key step for the success in post-operative vision regain is the adequate intraocular lens (IOL) dioptric power determination, superseding the dioptric power of the crystalline lens along with the necessary power for the correction of inherent refractive errors and achievement of the targeted post-operative refraction. Astigmatism is highly prevalent in cataract patients, deteriorating visual acuity [2]. As regards refractive astigmatism, the posterior corneal astigmatism (PCA) was pointed out as the major source of error [3], and a prediction error equal or lower than 0.50 D, with toric IOL power calculations, has been shown to vary between 53.9% and 65.6% [4], and 35% to 75% [5]. Therefore and along with the increasing rate of performed cataract surgeries and patients demand of perfect refractive outcome, the improvement in precision of toric IOL power calculations is essential.

In this work the main aim was to explore refractive astigmatism prediction error improvement strategies in the ophthalmology context of cataract surgery. The approaches consisted in analyses out of different perspectives: construct linear regression nomograms relating keratometric and total corneal astigmatism measurements; analyze the variation of corneal astigmatism within a 3.0- and a 4.0 mm zone and its influence on the predicted residual refractive astigmatism; compare the error in refractive astigmatism considering a different number of

measurements acquired at different surgery-related stages for several measurement modalities; assess the influence of several biometric parameters in an exploratory study of linear and non-linear methods for keratometry and total corneal astigmatism optimization; and perform ray-tracing IOL power calculations simulations in different scenarios including different parameters.

2. Background

The eye can be regarded as an optical system: first the entering light from an infinite distance object reaches the cornea, the primary refractive surface with around 40 D of refractive power. Then the iris acts as an aperture that regulates the amount of light that passes the pupil to the crystalline lens. This focusing lens element, which holds the remaining refractive power of the eye (in total 60 D), turns the image upside down, before it is detected by the retina. And finally the brain processes the image, turning it such that a correct interpretation is possible.

Image errors, known as aberrations, occur in a real optical system degrading the image quality. Aberrations can be classified into chromatic and monochromatic. The first arise due to distinct light refraction for different wavelengths, while the second are only related to one wavelength. Monochromatic low-order aberrations (LOAs) include myopia, hyperopia and astigmatism, the most common refractive errors, while the high-order aberrations (HOAs) comprehend spherical aberration and coma, among others [6].

Astigmatism in the eye is due to asymmetries in the refractive surfaces, leading to power differences along meridians. Therefore, two principal meridians passing through the eye and perpendicular to the optic axis are considered: one for the maximal curvature/power and another for the minimal curvature/power. When these power directions are perpendicular, the astigmatism is termed regular and thus a LOA, otherwise it is defined as irregular arising from highly irregular corneal shapes, as in the keratoconus condition [6]. Regular astigmatism is mainly due to anterior corneal toricity, however the posterior corneal surface also contributes to the total astigmatism of the optical system. Due to the existing power difference, the horizontal and vertical light rays from a distant object are focused as two perpendicular lines forming a three-dimensional structure termed Sturm's Conoid. Along this interval, the blurred image assumes different shapes and directions [7]. The astigmatism is divided into subgroups according to the axis direction: With-the-Rule (WTR) with a steeper vertical meridian between 60° and 120°, as Against-the-Rule (ATR) with a horizontal steeper meridian between 0° and 30° or 150° and 180°, or as Oblique with the steepest meridian between 31° and 59° or 121° and 149°.

Keratometry measurements are confined to an approximately 3.0 mm diameter central area of the cornea, assuming that the cornea is symmetric with two main meridians 90° apart. Furthermore, only the anterior corneal curvature is measured and the standard keratometric index, a fictitious index of usually 1.3375 is used to include the effect of the posterior corneal surface in the conversion to total corneal power. Corneal topography and tomography consider a larger corneal zone for acquiring measurements. Topography only measures the anterior corneal surface, while tomography analyses the whole cornea, providing information of the anterior and posterior surfaces [8]. Different measuring devices have different underlying techniques, briefly: the Aladdin® (Topcon, Tokyo, Japan) is a Placido disc-based optical biometer and topographer; Lenstar® LS 900 (Haag-Streit AG, Köniz, Switzerland) is an optical low-coherence reflectometry biometer; the Cassini® (i-Optics, Den Haag, The Netherlands) is a topographer employing multi-colored LED point-to-point forward ray-tracing; the Pentacam® (Oculus Optikgeräte GmbH, Wetzlar, Germany) is a tomographer composed of a rotating Scheimpflug camera; and the MS-39® (Costruzione Strumenti Oftalmici, Florence, Italy) is an anterior segment optical coherence tomographer.

3. Methods

3.1. Regression nomograms

Pre-operative keratometric astigmatism (KA) measurements with Lenstar and total corneal astigmatism (TCA) measurements with Cassini were performed for patients scheduled to undergo cataract surgery. Only patients with measurements taken with both devices were considered, as well as with a criterion of 80 for the Cassini's quality factor of the posterior corneal surface. The KA and TCA measurements were decomposed into horizontal and vertical components following the Holladay *et al.* vector analysis [9] with double-angles by equations (1) and (2), where $Cylinder$ and $Axis$ are relative to the astigmatism magnitude and direction, respectively. For the whole sample and each of the three astigmatism subgroups, a linear regression was fitted, separately, between the horizontal and the vertical components.

$$x = Cylinder \times \cos(2 \times Axis) \tag{1}$$

$$y = Cylinder \times \sin(2 \times Axis) \tag{2}$$

Patients with pre-operative KA, axial length (AL), and anterior chamber depth (ACD) Lenstar measurements, that underwent cataract surgery, for

whom the power of the implanted toric IOL was known and the post-operative subjective refraction was recorded, were considered for the assessment of the prediction error. The nomograms were employed for Lenstar's KA adjustment and the correspondent predicted residual astigmatism (PRA) was calculated by vector analysis based on the Holladay *et at.* publications of 2001 and 1988 [9, 10], and the Fam and Lim meridional analysis [11]. The error in predicted residual astigmatism (EPA) was calculated using the Thibos *et al.* method [12] as the difference at the corneal plane between the post-operative refraction and the PRA. A vertex distance of 12.0 mm was considered to convert the subjective refraction at the spectacle plane to the corneal plane. The prediction error for the KA adjustment with the Abulafia-Koch formula was also calculated [13]. For the cases where the implanted toric IOL was known the prediction error was also calculated with the Barrett Toric Calculator [14], and cases where the powers of the IOL given by the Barrett Toric Calculator matched the implanted IOL powers were considered.

3.2. Corneal astigmatism variation within 3.0- and 4.0 mm zones

Total corneal refractive power (TCRP) pre-operative measurements taken with the Pentacam were considered from a 3.0 mm and a 4.0 mm diameter ring centered on the pupil axis. The eyes were divided into astigmatism subgroups according to the steepest meridian of the 3.0 mm zone, and the mean magnitude values were compared.

The differences between the 3.0- and 4.0-mm zone's astigmatism magnitude were divided into 0.25 D intervals. From the total number of eyes, 20% were randomly chosen for astigmatism differences between zones lower than 0.50 D, since this range held most of the cases, and including all eyes for differences higher than 0.50 D. For these eyes, the suggested toric IOL power for each TCRP zone values, according to the Næser-Savini Toric Calculator, was recorded [15]. The predicted residual refractive astigmatism correspondent to the toric IOL power determined to be implanted with TCRP values from the 3.0 mm zone was compared to the prediction for the same toric IOL power, but with TCRP values from the 4.0 mm zone.

3.3. Error in refractive astigmatism analysis

A retrospective study included patients undergoing cataract surgery with toric IOL implantation (Acrysof SN6ATx, Alcon Laboratories, Inc.) with three consecutive measurements performed with Pentacam and Aladdin with a quality specification of "OK". Post-operatively, namely at least one month after the surgery, three consecutive measurements were performed using the same devices; the patients' subjective refraction was recorded; and the IOL orientation was determined using a slit-lamp aligned with the IOL indentations.

Corneal astigmatism from four different measurement modalities was obtained regarding the rotating Scheimpflug camera case: KA, TCRP 3.0 mmm P/Z (TCA from a 3.0 mm zone centered on the pupil), TCRP 3.0 mm A/Z (TCA from a 3.0 mm zone centered on the apex), TCRP 4.0 mm P/Z (TCA from a 4.0 mm zone centered on the pupil). The PCA was also recorded. As the Aladdin Placido disc corneal topographer only measures the keratometry, solely KA was considered. In addition, AL, ACD, white-to-white (WTW), and Chord μ (angle kappa related) measurements were recorded.

According to the first pre-operative KA measurement taken with Pentacam, the cases were divided into the three astigmatism subgroups and for each measurement modality, except Pentacam's PCA, three sets of measurements were considered: only the first pre-operative measurement, the average of the three pre-operative measurements, and the average of the three post-operative measurements. Hereinafter, measurement modalities refer to Pentacam's KA, TCRP 3.0 mm P/Z, TCRP 3.0 mm A/Z and TCRP 4.0 mm P/Z, as well as Aladdin's KA, while measurement types refer to the average of three pre-operative measurements, only one pre-operative measurement, and the average of three post-operative measurements.

The analysis of astigmatism power was carried out applying Næser's polar value method [7]. The astigmatism magnitude and axis (M @ α), in a plus cylinder format, were transformed into two polar components, the net meridional power along a reference meridian ϕ, by equation (3), and the net torsional power over the meridian ϕ, by equation (4).

$$\begin{aligned} &Net\ meridional\ power\ along\ \phi = \\ &= KP(\phi) = M \times \cos(2 \times (\alpha - \phi)) \end{aligned} \tag{3}$$

$$\begin{aligned} &Net\ torsional\ power\ over\ \phi = \\ &= KP(\phi + 45) = M \times \sin(2 \times (\alpha - \phi)) \end{aligned} \tag{4}$$

These components can be reconverted into the net astigmatism format, by equations (5) and (6).

$$M = \sqrt{KP(\phi)^2 + KP(\phi + 45)^2} \tag{5}$$

$$\alpha = \arctan\left(\frac{M - KP(\phi)}{KP(\phi + 45)}\right) + \phi \tag{6}$$

Using equations (3) and (4), the error in refractive astigmatism (ERA) was calculated at the corneal plane following three main steps: the target corneal astigmatism (TCAst) was calculated by vector summation of the KA or TCA and the calculated surgical induced corneal astigmatism (SICA)

as the difference between the post- and the pre-operative KA/TCA; the target refractive astigmatism (TRA) was obtained by summation of the calculated TCAst and the IOL astigmatism (IA), having as reference meridian the steepest measured meridian; the ERA was then obtained by the vector difference between the post-operative refraction astigmatism (RA) at the corneal plane and the TRA. A vertex distance of 12.0 mm was considered to transform the subjective refraction at the spectacle plane to the corneal plane.

For the optimization of the pre-operative corneal astigmatism, back-calculations were performed to zero-out the meridional ERA component. The IOL toricity and SICA were subtracted from the subjective refraction. An exploratory study employing supervised machine learning (ML) including different sets of parameters — corneal astigmatism and direction, AL, ACD, WTW, and Chord μ — was carried out aiming to assess the influence of the different parameters on the optimization process, using different linear and non-linear estimators from the scikit-learn library in Python 3.7 (Anaconda). Since the output was a quantitative prediction and therefore considered as a regression problem, and given the small volume of data, Multiple Linear Regression (Linear), Linear Support Vector Regression (SVR), K-Nearest Neighbor (KNN), Random Forest (RF), and Gradient Boosting (GB) estimators were considered. The whole sample, without subgroup distinction, was considered in a three-step analysis: step 1, using the whole sample for both, training and testing, termed Training; step 2, a k-fold cross-validation, to predict the estimators performance when unknown data is used for testing purposes, where the sample is split into k smaller sets, for which the estimator models are fitted and the performance is evaluated, being the total performance the average of the k-fold performances, termed Cross-validation; step 3, using this sample for training and testing with another independent sample, termed Testing.

3.4. **Ray-tracing IOL power calculations**

Pre-operative measurements performed with Pentacam for patients that underwent cataract surgery with toric IOL implantation (Acrysof SN6ATx, Alcon Laboratories, Inc.) were cross-referenced with post-operative measurements performed with MS-39, to assess the position of the implanted toric IOL. For these patients the parameters considered were: pre-operative corneal topography (radii of curvature, axis, and asphericity), AL, lens thickness (LT), pupil diameter (PD), WTW, and ACD; post-operative (one month after the surgery) corneal topography and the position of the implanted IOL (ACD_{postop}) as the distance from the corneal endothelium to the anterior surface of the implanted IOL. Additionally, one month after the surgery, the subjective refraction and IOL axis of implantation were recorded.

Adapted from the Personalized Pseudophakic Eye Model (PPM) developed by Ribeiro *et al.* [16], and based on the Liou-Brennan model [17], an astigmatic pseudophakic eye model was developed, suitable to incorporate patient-specific data, and to overcome the lack of information regarding IOLs disclosed by the manufacturers, a generic simulated toric IOL was conceptualized.

Three models were considered: two pre-operative, combined with formulas for the IOL position estimation, one PPM-based ($ACD_{post} = ACD_{pre} + 0.395 \times LT_{pre}$) [16], and a C-Constant concept ($IOL_C = ACD_{pre} + C \times LT_{pre}$, with a C-value of 0.38) [18]; and a post-operative, for which the IOL position was known.

3.5. **Statistical Analysis**

Statistical analysis was performed using the scipy.stats module of Python 3.7 (Anaconda). To assess if a sample followed a normal or Gaussian distribution, the Shapiro-Wilk statistical test was performed. Two paired samples were compared regarding statistical differences, using paired t-tests when normally distributed, and Wilcoxon signed-rank test when not normally distributed. When comparing three or more normal-distributed and paired samples, repeated measures analysis of variance (ANOVA) was used, and the Friedman non-parametric test for the case where the paired samples did not follow a Gaussian distribution. For all statistical tests a p-value of less than 0.05 was considered significant.

4. Results and Discussion

4.1. **Regression Nomograms**

Four nomograms were constructed by modeling linear correlations based on Lenstar's KA and Cassini's TCA, a generic nomogram considering all eyes (637) and astigmatism subgroup specific nomograms (WTR, 273 eyes; ATR, 255 eyes; Oblique, 109 eyes). These suggest a tendency to turn the horizontal WTR component less negative, while turning more positive the ATR one.

The mean±SD values for the EPA horizontal (x), net astigmatism magnitude and direction, and the percentage of eyes with an EPA magnitude lower or equal than 0.50 D are presented in Table 1 for the case with and without the generic and subgroup specific adjustments for the whole sample (175 eyes) and for the WTR (75 eyes) and ATR (85 eyes) subgroups. These parameters are also presented for the Abulafia-Koch Formula case [13].

Table 1: EPA horizontal (x) component, in D, correspondent net astigmatism, in D and °, and percentage of eyes with an EPA magnitude within 0.50 D. AK stands for Abulafia-Koch Formula.

	EPA, x	EPA, Net Ast.	% ≤0.50 D
Total			
Without	0.22±0.64	0.22 @ 177.1	44.00
Generic	0.05±0.65	0.05 @ 174.1	56.00
Specific	0.10±0.56	0.10 @ 174.9	52.57
AK	-0.17±0.55	0.17 @ 91.5	51.43
WTR			
Without	0.56±0.76	0.56 @ 0.1	26.67
Generic	0.19±0.64	0.19 @ 1.5	49.33
Specific	0.25±0.72	0.25 @ 2.0	44.00
AK	0.04±0.62	0.05 @ 20.4	53.33
ATR			
Without	-0.06±0.40	0.06 @ 90.7	56.47
Generic	-0.08±0.41	0.08 @ 90.2	60.00
Specific	-0.03±0.39	0.03 @ 87.9	58.82
AK	-0.39±0.42	0.39 @ 90.3	45.88

The centroid for the horizontal component overall decreased when KA is adjusted, with an WTR shift tendency, more pronounced for the Abulafia-Koch formula. The generic KA adjustment led to the largest decreases, with statistical significance ($p<0.001$), for both, total and WTR, cases. Despite the high number of ATR cases in the test sample, no statistical differences were found, what may be related to the already low prediction errors without adjustment. The percentage of eyes with an EPA magnitude lower or equal than 0.50 D increased when the KA was adjusted, namely with the generic nomogram, and similar to the Abulafia-Koch case for the whole sample. The differences with respect to the WTR and ATR subgroup between the nomogram cases and the Abulafia-Koch case may be related to the observed WTR shift of the EPA horizontal component when the Abulafia-Koch is employed, which leads to better outcomes for the WTR subgroup, but worse in relation to the ATR subgroup.

The prediction error was calculated with the Barrett Toric Calculator for 60 eyes. The horizontal centroid component correspondent to the case without adjustment (0.19±0.48 D) decreased for the adjustment cases with the generic (0.01±0.41 D) and specific (0.02±0.42 D) nomograms, as well as for the Barrett Calculator (0.11±0.32 D). The Abulafia-Koch Formula had a pronounced associated deviation towards WTR (-0.19±0.42 D). The magnitude and direction for the case without adjustment were 0.19 D @ 7.0°, while for the generic and specific nomograms adjustment cases these were, respectively, 0.06 D @ 40.2° and 0.05 D @ 34.2°. With the Abulafia-Koch Formula, these were 0.20 D @ 80.3° and with the Barrett Toric Calculator 0.12 D @ 175.6°. The lowest prediction error ($p<0.001$) and the highest percentage of eyes with a prediction error equal or lower than 0.50 D (88.33%) were obtained with the Barrett Toric Calculator — without adjustment the percentage was only 48.33%. Also, the nomogram adjustments led to a statistically significant decrease of the prediction error ($p=0.0036$ for the generic, and $p=0.0018$ for the specific nomogram cases) with correspondent percentages of prediction error lower or equal than 0.50 D of 56.67% and 61.67%.

4.2. Corneal astigmatism variation within 3.0- and 4.0 mm zones

The TCRP mean±SD values for the 3.0- and 4.0-mm zones for all eyes were, respectively, 1.15±0.83 D and 1.14±0.84 D. For the WTR subgroup these were, respectively, 1.23±0.80 D and 1.25±0.84 D, and for the ATR subgroup 1.19±0.88 D and 1.12±0.84 D. An average increase of the astigmatism is observed for the WTR subgroup, while for the ATR an average decrease.

Comparing the suggested toric IOL to be implanted based on the TCRP values of the 3.0 mm zone to the ones of the 4.0 mm zone, the power changed in 76.80% of the eyes, whereas 52.08% from these had lower toric IOL powers in the 4.0 mm zone than in the 3.0 mm zone, and 47.92% higher powers. Separating the astigmatism differences between zones in intervals of 0.25 D, the Mean Absolute Erros (MAE) was calculated between the predicted residual refractive astigmatism of the 3.0- and 4.0 mm zones, for the toric IOL power determined for the 3.0 mm zone. For differences below 0.25 D, the MAE was 0.08, while for differences between 0.25-0.50 D and 0.50-0.75 D it was 0.26 and 0.41, respectively. Regarding higher difference intervals also the MAE increased: between 0.75-1.0 D, the MAE was 0.75, surpassing 1.0 for differences higher than 1.0 D (MAE = 1.09). Except for astigmatism differences lower or equal than 0.25 D, in general, the prediction differences had values of the same order of magnitude as the correspondent interval of astigmatism differences.

4.3. Error in refractive astigmatism analysis

For each measurement modality and type, the mean±SD values for the ERA meridional component, as well as the MAE for the net astigmatism magnitude, and the percentage of eyes with an ERA magnitude equal or less than 0.50 D are presented in Table 2 for the WTR (54 eyes) and ATR (31 eyes) subgroups.

Table 2: Mean±SD values, in D, ERA meridional component, KP(ϕ), MAE for the net astigmatism magnitude, in D, and the percentage of eyes with an ERA magnitude equal or less than 0.50 D. The p-values refer to the differences between measurement types.

	WTR				**ATR**			
	KP(ϕ)	MAE	p	% $\leq$0.50D	KP(ϕ)	MAE	p	% $\leq$0.50D
KA (Pentacam)								
Average 3 preop	-0.53±0.41	0.67		33.33	0.32±0.31	0.60		38.71
1 preop	-0.54±0.48	0.67	0.7860	44.44	0.32±0.32	0.65	0.7892	29.03
Average 3 postop	-0.54±0.40	0.67		31.48	0.26±0.27	0.59		41.94
KA (Aladdin)								
Average 3 preop	-0.52±0.41	0.64		42.59	0.24±0.34	0.55		48.39
1 preop	-0.52±0.43	0.67	0.7034	38.89	0.25±0.36	0.57	0.6790	45.16
Average 3 postop	-0.52±0.34	0.65		35.19	0.21±0.34	0.52		51.61
TCRP 3.0 P/Z								
Average 3 preop	-0.15±0.42	0.49		59.26	0.22±0.39	0.59		38.71
1 preop	-0.17±0.46	0.52	0.1145	59.26	0.15±0.46	0.65	0.4274	35.48
Average 3 postop	-0.21±0.39	0.52		52.41	0.10±0.32	0.55		48.39
TCRP 3.0 A/Z								
Average 3 preop	-0.36±0.40	0.55		51.85	0.08±0.37	0.55		45.16
1 preop	-0.38±0.51	0.59	0.4111	50.00	0.06±0.36	0.60	0.7233	41.94
Average 3 postop	-0.39±0.36	0.56		50.00	0.01±0.35	0.55		45.16
TCRP 4.0 P/Z								
Average 3 preop	-0.27±0.36	0.51		55.56	0.23±0.35	0.57		48.39
1 preop	-0.30±0.43	0.54	0.9286	50.00	0.20±0.42	0.61	0.6449	41.94
Average 3 postop	-0.32±0.38	0.53		53.70	0.12±0.33	0.54		48.39

An overall over-correction (negative ERA KP(ϕ) values) was found for the WTR, while an under-correction (positive ERA KP(ϕ) values) for the ATR case, regarding all measurements of all modalities. Within each measurement modality, between the three different measurement types, no statistically significant differences were found regarding the ERA meridional polar values, and the ERA magnitude. Even if not statistically different, for most cases, the highest spread was observed for the one pre-operative measurement case, and the lowest percentage of eyes with an error lower or equal to 0.50 D for the average of three post-operative measurements.

The TCRP cases have a higher dispersion compared to the KA cases, however, these measurement modalities led to a decrease of the observed over- and under-correction: the ERA KP(ϕ) is closer to zero when compared to the KA cases, what suggests that it is more accurate. Furthermore, this decrease is related to the posterior corneal effect of WTR KA compensation, on the one hand, and of the ATR KA adding effect, on the other [19]. When comparing the ERA meridional and torsional components between measurement modalities, the TCRP cases covering a 3.0 mm zone centered on the pupil provided the best outcomes for the WTR case, while the centered on the apex led to the best outcomes for the ATR case.

In the optimization method analysis, the best achievable outcomes are limited by the back-calculated outcomes, namely a mean±SD zero meridional ERA and a percentage of 76% eyes with an ERA within 0.50 D. The torsional ERA is not optimized by back-calculations, therefore remaining unchanged between non-optimized and optimized. The net astigmatism calculated with the Barrett Toric Calculator led to a mean±SD value, in D, for the ERA KP(ϕ) of 0.12±0.40, and 50% of eyes with an ERA magnitude equal or lower than 0.50 D.

In Figure 1 are presented for the Pentacam KA case the ERA meridional and torsional components with 95% confidence ellipses for all estimators. The centroid is approximately zero for all cases, and the ellipses narrow towards zero along the $xx-$ axis, when considering more parameters, being less pronounced for the linear and KNN estimators. Regarding the ellipse axes along the horizontal component, they are lower for the three-based estimators, therefore showing lower variance and higher precision when compared to the linear estimators. Percentages around 60% were achieved with the Linear, Linear SVR, and KNN estimators for ERA magnitude values $\leq$0.50 D, while higher than 70% for the RF and GB estimators.

Through statistical analysis, in the KA cases the mean ERA KP(ϕ) and magnitude components were lower compared to the non-optimized case ($p<0.05$

and p<0.001, for the meridional and magnitude components). When comparing the optimization estimators with the Barrett Toric Calculator case, the optimized mean ERA meridional components were lower (p<0.05) and, overall, for the ERA magnitude no statistical differences were found for the linear estimators; however, statistically lower mean values were found for the RF and GB cases. The linear estimators had as well higher values compared to these two estimators. In general, regarding the mean meridional and magnitude ERA, no statistical differences were found when comparing the different parameter sets for the same estimator.

In the cross-validation step, higher R^2 scores, around 0.80, and lower SDs were found for the Linear and Linear SVR estimators, compared to the around 0.70 for the tree-based estimators, suggesting that when using unknown data to predict optimized corneal astigmatism values, the accuracy of the first estimators will be higher and with a smaller deviation than the tree-based estimators.

As the KNN estimator appeared to perform worse when considering more parameters, in the testing step were used only the Linear and Linear SVR regressions, as well as the RF and GB estimators. With 52 eyes in the testing phase, the mean±SD, for the ERA KP(ϕ) component, and the percentage of eyes with an ERA magnitude equal or lower than 0.50 D is presented in Table 3 for the Linear, Linear SVR, RF and GB estimators. The number 1 stands for the parameter set of astigmatism magnitude and direction; 2 includes also the AL and ACD; 3 includes, in turn, the Chord μ; and 4 includes all parameters.

Table 3: Mean±SD values, in D, ERA KP(ϕ), and the percentage of eyes with an ERA magnitude equal or less than 0.50 D, in the Testing phase.

	1	2	3	4
Linear				
KP(ϕ): Mean	-0.06	-0.05	-0.05	-0.04
KP(ϕ): SD	0.41	0.40	0.42	0.43
% ≤0.50D	51.92	51.92	50.00	48.08
SVR				
KP(ϕ): Mean	-0.10	-0.11	-0.09	-0.10
KP(ϕ): SD	0.40	0.40	0.41	0.41
% ≤0.50D	50.00	48.08	48.08	42.31
RF				
KP(ϕ): Mean	-0.02	-0.08	-0.03	-0.09
KP(ϕ): SD	0.42	0.48	0.42	0.49
% ≤0.50D	51.92	48.08	50.00	48.08
GB				
KP(ϕ): Mean	-0.03	-0.05	-0.01	-0.03
KP(ϕ): SD	0.46	0.46	0.50	0.49
% ≤0.50D	51.92	46.15	44.23	46.15

An overall over-correction is present, with a mean meridional ERA value close to zero. The mean values are lower for the tree-based estimators, but the SD values are lower for the linear estimators; the same results were found for the magnitude ERA case. In general, the percentage of eyes with an ERA magnitude equal or lower than 0.50 D rounds 50%. The highest percentages obtained by the estimators occur for the simple case where magnitude and direction of astigmatism were considered, whereas the percentages decrease when more parameters were included, however no statistical differences were found when comparing different parameter sets for one estimator.

4.4. **Ray-tracing IOL power calculations**

For each model, the mean±SD values were calculated for the spherical and cylindrical powers, their results being depicted in Table 4. In addition, the R^2 coefficients in relation to the implanted IOL powers were determined. The mean±SD spherical power of the implanted IOL was 19.24±3.53 D, and the cylindrical was 2.00±1.31 D.

Table 4: Mean±SD spherical and cylindrical powers for the three models, and R^2 with respect to the implanted toric IOL.

	Mean	SD	R^2
Preop + PPM			
Spherical	20.44	4.35	0.82
Cylindrical	2.04	1.82	0.84
Preop + C Const			
Spherical	20.33	4.30	0.82
Cylindrical	2.04	1.80	0.84
Postop			
Spherical	19.01	4.08	0.83
Cylindrical	2.06	1.86	0.84

The cylindrical power obtained using the three models did not statistically differ from the implanted IOL cylindrical power, and also in-between of them no differences were found, however these were, by observations, slightly higher than the cylindrical power of the implanted IOL. Regarding the spherical power, the mean values of the implanted IOL were similar to the obtained with the generic simulated IOL using the post-operative model, and statistically lower when compared to both pre-operative models (p<0.05).

For each of the three models, the prediction error was calculated as the difference between the recorded subjective refraction and the predicted post-operative refraction that was simulated, taking into account the biometric data and the known powers of the implanted IOL. For the post-operative model, the mean±SD difference was -0.59±0.85 D

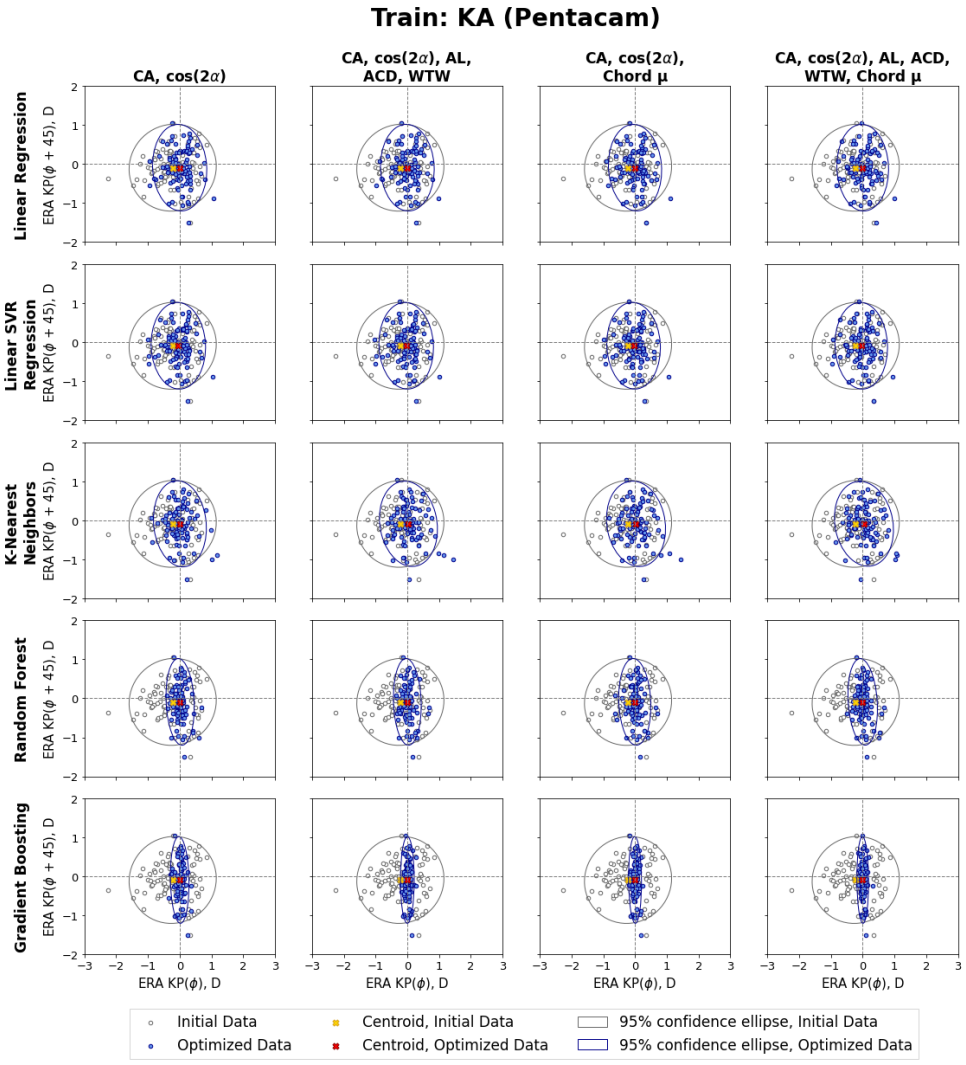

Figure 1:
ERA KP(ϕ) and KP(ϕ+45) components displayed by 95% confidence ellipses, for the optimized KA (Pentacam), in the Training stage.

for the spherical power and -0.37±0.33 D for the cylindrical power, while regarding the pre-operative model with the PPM-based formula, these were -1.42±0.84 D and -0.20±0.34 D, and with the C Constant -1.39±0.79 D and -0.21±0.34 D. The negative mean values indicate a higher refractive power of the generic simulated IOL, for which the refraction spherical power is higher for the pre-operative models, pointing out the influence of the effective IOL position. For the cylindrical power, the variation is small between models, i.e., below 0.50 D, and a percentage of 63.16% was attained for a prediction error equal or lower than 0.50 D, for all models.

By simulation of the effect of neglecting the PCA, the mean±SD cylindrical power changes are presented in Table 5 for the WTR (10 eyes) and ATR (6 eyes) subgroups.

The cylindrical power increased for the WTR eyes when not encountering the posterior surface, which is in line with the highlighted compensation influence of this surface on the anterior corneal surface. Therefore, when only considering the anterior corneal astigmatism the respective IOL power will be higher, related to the error in refractive astigmatism over-correction associated to this astigmatism subgroup. On the other hand, the IOL cylindrical power decreased for the ATR subgroup, which is related to the posterior corneal surface adding influence, meaning that when only considering the anterior corneal astigmatism the IOL power calculated will be lower than when considering both surfaces, leading to the characteristic error in refractive astigmatism under-correction of the ATR subgroup.

5. Conclusions

The KA nomogram adjustment reflected a significant reduction of the prediction error in residual astigmatism, increasing the percentage of eyes with a prediction error within 0.50 D from 44% to 56% when adjusted by the generic nomogram. An over-

Table 5: Mean±SD values, in D, for the cylindrical powers of the three simulated models when and when not considering the posterior corneal astigmatism, for the WTR and ATR subgroups.

	WTR	ATR
With PCA		
Preop + PPM	2.65±2.01	0.97±0.59
Preop + C-Constant	2.64±2.00	0.97±0.59
Postop	2.84±1.95	0.85±0.69
Without PCA		
Preop + PPM	2.91±2.07	0.71±0.5)
Preop + C-Constant	2.89±2.06	0.81±0.54
Postop	3.03±2.01	0.72±0.60

all shift towards WTR was depicted, in line with other adjustment methods. Nevertheless, an enhancement of the developed nomograms may be necessary for the reduction of the outlier cases and for the increase of the correlation coefficient between the measured KA and TCA.

Focusing on further possible factors that should be considered, the present study about TCA from a 4.0 mm zone compared to the 3.0 mm zone pointed out that at least slight variations existed between them, namely for the ATR subgroup. Higher variations were in line with an increase of the predicted residual refractive astigmatism difference between zones, which may produce an impact on refractive outcomes. Conversely, it was shown that by considering the average of three pre-operative measurements or solely one pre-operative measurement did not reflect differences in the error in refractive astigmatism across different measurement modalities, even when compared to the average of three post-operative measurements.

The exploratory study about the employment of linear and non-linear machine learning estimators for the optimization of the pre-operative KA and TCA highlighted their potential to reduce the error in refractive astigmatism, attaining percentages of eyes with an error in refractive astigmatism equal or lower than 0.50 D as high as 75%, in the training step. However, more recent datasets should be used in future studies to test the estimators combined with several other biometric parameters and also the possibility of adaptation of the machine learning algorithms.

The developed astigmatic pseudophakic eye model along with the generic simulated toric IOL for ray-tracing power calculations, necessarily created to overcome the lack of lens specificities, provided the major advantages for being suitable for patient-specific data incorporation, and moreover they do not depend on previous population data for IOL power calculations. The model's limitations are the unavoidable pre-operative lens position estimation and the inherent biometric measurements accuracy. The implementation of this model for IOL power ray-tracing calculations striked the potential not only of the model and toric IOL concept, but also of the method for the improvement of refractive outcomes, highlighting their versatility for the study of several scenarios regarding the challenging issue of post-operative IOL physical position estimations and the cylindrical power relation to the posterior cornea encountering. More simulations, including more eyes, with the generic simulated toric IOL should be performed to give strength to this concept and point out the adaptations needed. Alternative optimization methods need to be further studied as well as methods for the assessment of the refraction to determine more accurately the prediction error.

In essence, the main contributions of the conducted studies rely on the distinct improvement strategies to overcome some of the highlighted sources of error and exploit other possible factors to be taken into account for the improvement of refractive outcomes, pointing out that future studies require mainly a global inclusion of larger numbers of eyes to sustain the found results and enable more robust conclusions.

Acknowledgements

This document was written and made publically available as an institutional academic requirement and as a part of the evaluation of the MSc thesis in Biomedical Engineering of the author at Instituto Superior Técnico. The work described herein was performed at the Institute for Plasmas and Nuclear Fusion of Instituto Superior Técnico (Lisbon, Portugal), during the period February-November 2021, under the supervision of Prof. Dr. João Mendanha Dias, and co-supervision of Prof. Dr. Filomena Ribeiro (Hospital da Luz Lisboa, Lisbon, Portugal), continuing the research work started in July 2019. In addition, during the period May-July 2021, an internship was performed at the Studio Oculistico D'Azeglio (Bologna, Italy), under the supervision of Dr. Giacomo Savini, and co-supervised at Instituto Superior Técnico by Prof. Dr. João Mendanha Dias.

References

[1] Y.-C. Liu, M. Wilkins, T. Kim, B. Malyugin, and J. S. Mehta. Cataracts. *Lancet*, 390(10094):600–612, August 2017. doi:10.1016/S0140-6736(17)30544-5.

[2] T. Ferrer-Blasco, R. Montés-Micó, S. C. P. de Matos, J. M. González-Méijome, and A. Cerviño. Prevalence of corneal astigmatism before cataract surgery. *Journal of Cataract*

and Refractive Surgery, 35(1):70–75, January 2009. doi:10.1016/j.jcrs.2008.09.027.

[3] G. Savini and K. Næser. An Analysis of the Factors Influencing the Residual Refractive Astigmatism After Cataract Surgery With Toric Intraocular Lenses. *Investigate Ophthalmology & Visual Science*, 56(2):827–835, February 2015. doi:10.1167/iovs.14-15903.

[4] J. X. Kane and B. Connell. A Comparison of the Accuracy of 6 Modern Toric Intraocular Lens Formulas. *Ophthalmology*, 127(11):1472–1486, November 2020. doi:10.1016/j.ophtha.2020.04.039.

[5] T. B. Ferreira, P. Ribeiro, F. J. Ribeiro, and J. G. O'Neill. Comparison of methodologies using estimated or measured values of total corneal astigmatism for toric intraocular lens power calculation. *Journal of Refractive Surgery*, 33(12):794–800, December 2017. doi:10.3928/1081597X-20171004-03.

[6] E. Hecht. *Optics*. Addison-Wesley, fourht edition, 2001.

[7] K. Næser. Assessment and statistics of surgically induced astigmatism. *Acta ophthalmologica*, 86:349, June 2008. Thesis.

[8] M. Corbett, N. Maycock, E. Rosen, and D. O'Brart. *Corneal Topography*. Springer International Publishing, second edition, 2019. doi: 10.1007/978-3-030-10696-6.

[9] J. T. Holladay, J. R. Moran, and G. M. Kezirian. Analysis of aggregate surgically induced refractive change, prediction error, and intraocular astigmatism. *Journal of Cataract and Refractive Surgery*, 27(1):61–79, January 2001. doi:10.1016/s0886-3350(00)00796-3.

[10] J. T. Holladay, T. C. Prager, T. Y. Chandler, K. H. Musgrove, J. W. Lewis, and R. S. Ruiz. A three-part system for refining intraocular lens power calculations. *Journal of Cataract and Refractive Surgery*, 14(1):17–24, January 1988. doi:10.1016/s0886-3350(88)80059-2.

[11] H. B. Fam and K. L. Lim. Meridional analysis for calculating the expected spherocylindrical refraction in eyes with toric intraocular lenses. *Journal of Cataract and Refractive Surgery*, 33(12):2072–2076, December 2007. doi:10.1016/j.jcrs.2007.07.034.

[12] L. N. Thibos, W. Wheeler, and D. Horner. Power vectors: an application of fourier analysis to the description and statistical analysis of refractive error. *Optometry and Vision Science*, 74(6):367–375, June 1997. doi:10.1097/00006324-199706000-00019.

[13] A. Abulafia, D. D. Koch, L. Wang, W. E. Hill, E. I. Assia, M. Franchina, and G. D. Barrett. New regression formula for toric intraocular lens calculations. *Journal of Cataract and Refractive Surgery*, 42(5):663–671, May 2016. doi:10.1016/j.jcrs.2016.02.038.

[14] Barrett Toric Calculator (Version 2.0). https://ascrs.org/tools/barrett-toric-calculator. Accessed: 2021-10-25.

[15] Naeser/Savini Toric Calculator Version 1.2.4. https://www.sedesoi.com/toric-2021/. Accessed: 2021-10-26.

[16] F. J. Ribeiro, A. Castanheira-Dinis, and J. M. Dias. Personalized Pseudophakic Model for Refractive Assessment. *PLoS One*, 7(10):e46780, October 2012.

[17] H.-L. Liou and N. A. Brennan. Anatomically accurate, finite model eye and optical modelling. *Journal of the Optical Society of America A*, 14(8):1684–1695, 1997. doi:10.1364/JOSAA.14.001684.

[18] T. Olsen and P. Hoffmann. C constant: new concept for ray tracing-assisted intraocular lens power calculation. *Journal of Cataract and Refractive Surgery*, 40(5):764–773, May 2014. doi:10.1016/j.jcrs.2013.10.037.

[19] G. Savini, K. Næser, D. Schiano-Lomoriello, and P. Ducoli. Optimized keratometry and total corneal astigmatism for toric intraocular lens calculation. *Journal of Cataract and Refractive Surgery*, 43(9):1140–1148, September 2017. doi:10.1016/j.jcrs.2017.06.040.